Sparse Regression Codes for Integrated Passive Sensing and Communications

Chenghong Bian, Kaitao Meng, Huihui Wu, Deniz Gündüz

Abstract—We propose a novel integrated sensing and communication (ISAC) system, where the base station (BS) passively senses the channel parameters using the information carrying signals from a user. To simultaneously guarantee decoding and sensing performance, the user adopts sparse regression codes (SPARCs) with cyclic redundancy check (CRC) to transmit its information bits. The BS generates an initial coarse channel estimation of the parameters after receiving the pilot signal. Then, a novel iterative decoding and parameter sensing algorithm is proposed, where the correctly decoded codewords indicated by the CRC bits are utilized to improve the sensing and channel estimation performance at the BS. In turn, the improved estimate of the channel parameters lead to a better decoding performance. Simulation results show the effectiveness of the proposed iterative decoding and sensing algorithm, where both the sensing and the communication performance are significantly improved with a few iterations. Extensive ablation studies concerning different channel estimation methods and number of CRC bits are carried out for a comprehensive evaluation of the proposed scheme.

Index Terms—Sparse regression code, Integrated sensing and communication (ISAC), Iterative decoding.

I. INTRODUCTION

Integrated sensing and communications (ISAC) has been gaining significant research interest [1]–[3]. ISAC can significantly enhance spectrum and energy efficiency, reducing the hardware costs and addressing bandwidth congestion problems in upcoming 6G networks. ISAC systems can be catagorized as active or passive sensing. In ISAC with active sensing, the transmitter (typically the BS) transmits both the sensing signal and the information carrying signal, and utilizes the echo signal to estimate the parameters of interest [1]. In passive sensing, on the other hand, the BS uses the signals it receives from the users to perform joint sensing and decoding without transmitting signals of its own [4], [5].

Existing studies rarely address channel coding in ISAC systems, focusing instead on theoretical bounds on the mean square error (MSE) of the estimated parameters and the achievable communication rate [1], [2]. In practice, these communication rates cannot be realized without the implementation of channel codes [6], [7]. Exploring this, the authors in [6] reveal the fact that satisfactory (active) sensing performance can be achieved if the low density parity check (LDPC)-coded signals are utilized for sensing. In [7], the authors first show that sparse vector coding (SVC) can be a good candidate for active
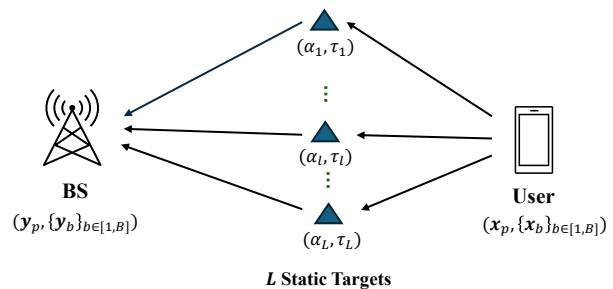
C. Bian and D. Gündüz are with the Department of Electrical and Electronic Engineering, Imperial College London (E-mails: {c.bian22, d.gunduz}@imperial.ac.uk). K. Meng is with the Department of Electronic and Electrical Engineering, University College London, London, UK (email: kaitao.meng@ucl.ac.uk). H. Wu is with RDA Technologies Limited, Hong Kong, China (email: huihui.wu@ieee.org).

Fig. 1: In the considered passive ISAC scenario, the user transmits both pilot and data packets to the BS under the OFDM framework. We assume L static targets/scatterers, where the l-th one, $l \in [1, L]$, is associated with a delay τ_l and a complex gain α_l.

sensing as the ambiguity function of the SVC signal has less significant side lobes compared with the uncoded signal. They then show that SVC outperforms convolutional codes in both error correction ability and sensing performance. However, both works focus on active sensing and to the best of our knowledge, no prior work considers coded passive sensing under the ISAC framework. The most relevant works are [4] and [5] where both consider transmitting uncoded QAM symbols. In particular, in [5], the authors adopt a Transformer-based neural network to first decode the QAM symbols and the decoded symbols are used for parameter sensing. However, as the QAM symbols are uncoded and a considerable amount of symbol errors may occur even under a relatively high SNR, the symbol errors will degrade the sensing performance, which further hinders the subsequent communication performance. Similar analysis applies for [4] as well, although the authors propose advanced learning-based iterative data detection and sensing algorithm to improve the system performance, the framework can be further strengthened with the aid of channel coding.

In this paper, we implement the first integrated passive sensing and communication system using coded signals in the orthogonal frequency division multiplexing (OFDM) framework. We start from a simplified setup where both the user and the BS have only one antenna and the scatters are assumed to be static. The cyclic redundancy check (CRC)-aided sparse regression code [8] with a K-best decoding algorithm proposed in [9] is adopted due to its superior performance for short packet transmission [10], [11]. The user transmits both the pilot and the coded data packets to the BS over a multi-path fading channel, and the BS performs iterative sensing and decoding.

The iteration starts with initial channel estimation using the received pilot signal. However, the coarse initial channel estimate from the pilot signal can be insufficient to achieve a satisfactory decoding performance. To this end, we first apply the K-best decoding algorithm to each of the received data packets using the estimated channel in the previous iteration. The decoder outputs the decoded bit sequence as well as an error flag indicating whether the decoded bit sequence passes the CRC, for each of the received codewords. The decoded bit sequences that pass the CRC will be used for the subsequent parameter sensing and channel estimation steps to provide more accurate estimates. It is shown in our experiments that both the sensing and communication performance can be significantly improved within a few iterations. Extensive simulations are carried out to evaluate the packet error rate (PER) performance and the sensing MSE of the proposed iterative ISAC algorithm. The superiority of SPARC over the Polar coded and uncoded baselines is also verified.

II. SYSTEM MODEL

A. Pilot and Data Transmission

We consider the passive ISAC scenario depicted in Fig. 1. We assume N OFDM subcarriers, each occupying a bandwidth of ΔB. The pilot signal, denoted by $\boldsymbol{x}_p \in \mathbb{C}^N$ in the frequency domain, is transmitted by the user over the multi-path channel. We assume there exist L static targets/scatterers in the environment[1], whose time domain channel response can be expressed as:

$$h(t) = \sum_{l=1}^{L} \alpha_l \delta(t - \tau_l), \tag{1}$$

where α_l and τ_l denote the complex gain containing the radar cross section (RCS) of the l-th target, and the delay corresponding to the l-th path, respectively. It is worth emphasizing that τ_l is a multiple of $\frac{1}{\Delta B}$, i.e., $\tau_l = n_l \frac{1}{\Delta B}, n_l \in [1, N_G]$, where N_G is the guard interval of the OFDM symbol, and typically we have $N_G = N/4$. The received pilot signal in the frequency domain can be expressed as:

$$\boldsymbol{y}_p = \boldsymbol{h} \odot \boldsymbol{x}_p + \boldsymbol{w}_p, \tag{2}$$

where $\boldsymbol{h} \in \mathbb{C}^N$ is the frequency domain response of $h(t)$ in (1), $\odot$ represents element-wise multiplication and $\boldsymbol{w}_p \in \mathcal{CN}(\boldsymbol{0}, \sigma_p^2 \boldsymbol{I}_N)$ denotes the AWGN. The SNR of the pilot signal is defined as $\text{SNR}_p \triangleq \frac{\mathbb{E}(\|\boldsymbol{x}_p\|_2^2)}{\mathbb{E}(\|\boldsymbol{w}_p\|_2^2)} = 1/\sigma_p^2$ as we assume $\mathbb{E}(\|\boldsymbol{x}_p\|_2^2) = N$.

The estimated channel, $\hat{\boldsymbol{h}}$, can be obtained from the received pilot, $\boldsymbol{y}_p$ via linear minimum mean square error (LMMSE) channel estimation:

$$\hat{\boldsymbol{h}} = \boldsymbol{R}_h (\boldsymbol{R}_h + \sigma_p^2 (\boldsymbol{x}_p \boldsymbol{x}_p^\dagger)^{-1})^{-1} \boldsymbol{y}_p / \boldsymbol{x}_p, \tag{3}$$

where $\boldsymbol{R}_h \triangleq \mathbb{E}_{\boldsymbol{h}}(\boldsymbol{h}\boldsymbol{h}^\dagger)$ denotes the covariance matrix of the channel frequency response.

The data packet contains information bit sequence, $\boldsymbol{b} \in \{0,1\}^{N_b}$, which is coded and modulated to generate $\boldsymbol{x}_d \in \mathbb{C}^N$.

[1]We leave the study of the mobile scenario as a future work.

The modulated codeword is transmitted over the same channel[2] with the same channel state information (CSI), $\boldsymbol{h}$, in (2). We detect and decode the information bit sequence using the estimated channel, $\hat{\boldsymbol{h}}$. In particular, MMSE channel equalization is adopted to generate the log likelihood ratio (LLR) values for each coded bit followed by channel decoder to produce the final decoded bit sequence, $\hat{\boldsymbol{b}}$. The equalization and decoding processes are standard and we skip them due to the page limit. The packet error rate (PER) of the system can be defined as:

$$\text{PER} = \mathbb{E}[\mathbf{1}(\boldsymbol{b} \neq \hat{\boldsymbol{b}})], \tag{4}$$

where $\mathbf{1}(\cdot)$ denotes the indicator function, which is 1 if the two-bit sequences are identical, and 0 otherwise.

B. Parameter Sensing

This subsection outlines the parameter estimation process in the considered ISAC system. Following the generally investigated parameter sensing scenario, we are interested in estimating $(\alpha_l, n_l), l \in [1, L]$, where the number of paths L is assumed to be known in advance at the BS[3]. These two parameters are essential for characterizing the environment and the objects within it, while the estimated values can also be leveraged to reconstruct the communication channel, and as a result, to enhance the reliability of data transmission.

Based on the estimated channel $\hat{\boldsymbol{h}}$ in (3), we apply inverse fast Fourier transform (IFFT) to convert it into the discrete time-domain response, i.e., $\hat{\boldsymbol{h}}^t = \text{IFFT}(\hat{\boldsymbol{h}})$. The estimated $(\hat{\alpha}_l, \hat{n}_l)$ denote the complex gain and the index of the element whose amplitude is the l-th largest in $\hat{\boldsymbol{h}}^t$:

$$\begin{aligned} \{\hat{n}_l\}_{1:L} &= \text{topL}(|\hat{\boldsymbol{h}}^t|), \\ \hat{\alpha}_l &= \hat{\boldsymbol{h}}^t[\hat{n}_l], \quad \forall l \in [1, L], \end{aligned} \tag{5}$$

where $\text{topL}(\boldsymbol{x})$ outputs the indices of the top-L values of $\boldsymbol{x}$. The reconstructed time domain response, $\hat{\boldsymbol{h}}_r^t \in \mathbb{C}^N$, can be expressed as:

$$\hat{\boldsymbol{h}}_r^t[n] = \begin{cases} \hat{\alpha}_l, & n = \hat{n}_l, \\ 0, & \text{otherwise.} \end{cases} \tag{6}$$

The sensing performance is evaluated by calculating the MSE between $\hat{\boldsymbol{h}}_r^t$ and the ground truth, $\boldsymbol{h}^t \triangleq \text{IFFT}(\boldsymbol{h})$:

$$\text{MSE} = \mathbb{E}(\|\hat{\boldsymbol{h}}_r^t - \boldsymbol{h}^t\|_2^2). \tag{7}$$

III. THE PROPOSED CODED ISAC SYSTEM

In this section, we will first illustrate the encoding and decoding processes of the proposed CRC-assisted SPARC over the considered multi-path fading channel. Then, the iterative decoding and sensing algorithm is presented, and shown to significantly improve both the communication and sensing performances.

[2]We assume the channel keeps constant for $B \geq 1$ data packets.

[3]If L is unknown, it can be determined by counting the number of taps which are above a predetermined threshold.
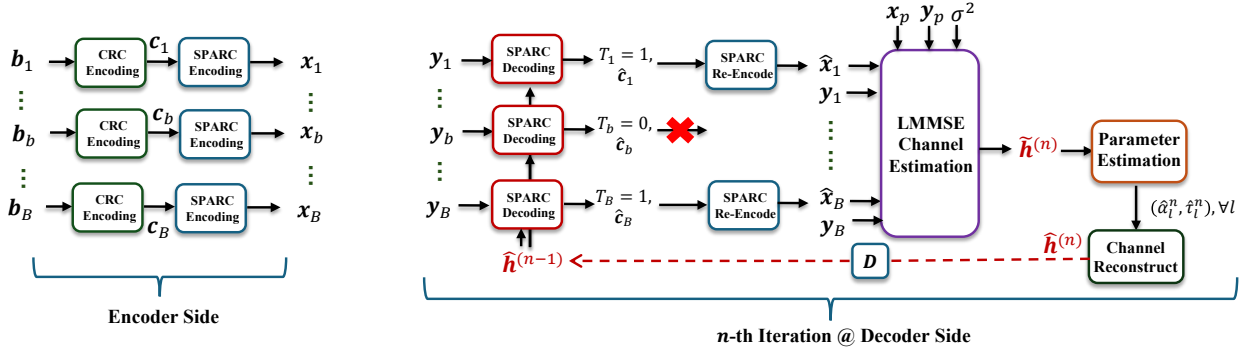
Fig. 2: Illustration of the proposed coded ISAC system. At the encoder, B bit sequences are CRC and SPARC encoded to generate the transmit signals. At the decoder, upon receiving the data packets $\boldsymbol{y}_b, b \in [1, B]$ as well as the pilot signal, $\boldsymbol{y}_p$, we run the proposed iterative decoding and sensing algorithm. In particular, for the n-th iteration, we apply the SPARC decoding algorithm which takes $\hat{\boldsymbol{h}}^{(n-1)}$ and $\boldsymbol{y}_b$ as input and outputs the decoded bits, $\hat{\boldsymbol{c}}_b$ and the CRC flag, T_b. The decoded bits $\hat{\boldsymbol{c}}_b$ with $T_b = 1$ are SPARC re-encoded for a refined channel and parameter estimation. Finally, we obtain the decoded bits, $\hat{\boldsymbol{c}}_b$ and the estimated sensing parameters, $(\hat{\tau}_l^{(N_i)}, \hat{\alpha}_l^{(N_i)}), \forall l \in [1, L]$ as output.

A. CRC-assisted SPARC for OFDM system

We consider the CRC-assisted SPARC due to its superior performance with respect to (w.r.t.) the state-of-the-art Polar codes for short packet transmission over AWGN and MIMO channels [9], [11]. The encoding and decoding of SPARC over an OFDM channel are detailed next.

1) CRC-assisted SPARC encoding: The encoding process is comprised of two parts, namely, the CRC and SPARC encoding. To start with, the input bit sequence, denoted by $\boldsymbol{b} \in \{0, 1\}^{V \log_2(M) - N_{crc}}$, is fed to the CRC encoding block where N_{crc} extra CRC bits are appended to $\boldsymbol{b}$ to produce a new bit sequence $\boldsymbol{c} \in \{0, 1\}^{V \log_2(M)}$ for the subsequent SPARC encoding. Then, we partition $\boldsymbol{c}$ into V blocks, each is comprised of $\log_2(M)$ bits[4]. The SPARC is characterized by its codebook, $\boldsymbol{\mathcal{C}} \in \mathbb{C}^{V \times M \times N}$, consisting of independent and identically distributed (i.i.d.) entries from the complex Gaussian distribution $\mathcal{CN}(0, 1/V)$. $\log_2(M)$ bits of the v-th block are mapped to an index, $m_v \in [1, M]$, which corresponds to the length-N sub-codeword, $\boldsymbol{\mathcal{C}}_v[m_v]$. By superposing all V sub-codewords, the transmitted codeword is obtained as:

$$\boldsymbol{x} = \sum_{v=1}^{V} \boldsymbol{\mathcal{C}}_v[m_v]. \tag{8}$$

We can easily verify that $\mathbb{E}(\boldsymbol{x}^\dagger \boldsymbol{x}) = N$ using the i.i.d. property of the elements within the codebook.

2) SPARC decoding: Then, we present SPARC decoding for an OFDM channel. We provide a brief overview of the decoding algorithm here, and refer the readers to [9] for more details.

Codebook update: We assume CSI, $\boldsymbol{h}$, is perfectly available at the decoder[5]. The codebook, $\boldsymbol{\mathcal{C}}$, is updated w.r.t $\boldsymbol{h}$ as:

$$\boldsymbol{\mathcal{C}}_{v,\boldsymbol{h}}[m] = \boldsymbol{h} \odot \boldsymbol{\mathcal{C}}_v[m], \quad \forall v \in [1, V], \forall m \in [1, M]. \tag{9}$$

---

[4]We assume M is a power of 2.

[5]The SPARC decoding algorithm is still valid when there is an estimation error in $\boldsymbol{h}$.

K-best decoding: We then illustrate the procedure to decode SPARC codeword with a K-best decoding algorithm. To be precise, the posterior probability of the SPARC codeword can be expressed as:

$$P(m_1, \ldots, m_V | \boldsymbol{y}, \boldsymbol{h}) \propto$$
$$\exp\{-\frac{1}{2\sigma^2} \|\boldsymbol{y} - \sum_{v=1}^{V} \boldsymbol{\mathcal{C}}_{v,\boldsymbol{h}}[m_v]\|_2^2\}. \tag{10}$$

The decoding objective is to find a combination of indices, $\{m_1, m_2, \ldots, m_V\}$ that maximizes (10). This is equivalent to minimizing the L2 distance, $\|\boldsymbol{y} - \sum_{v=1}^{V} \boldsymbol{\mathcal{C}}_{v,\boldsymbol{h}}[m_v]\|_2^2$.

Similarly [9], we define the *score metric*, $s^{(l)} = \|\boldsymbol{y} - \sum_{i=1}^{l} \boldsymbol{\mathcal{C}}_{i,\boldsymbol{h}}[m_i]\|_2^2$, which can be expressed recursively as:

$$s^{(l)} = s^{(l-1)} + \|\boldsymbol{\mathcal{C}}_{l,\boldsymbol{h}}[m_l]\|_2^2$$
$$+ 2\Re(\boldsymbol{\mathcal{C}}_{l,\boldsymbol{h}}^\dagger[m_l]\boldsymbol{u}^{(l-1)} - \boldsymbol{\mathcal{C}}_{l,\boldsymbol{h}}^\dagger[m_l]\boldsymbol{y}), \tag{11}$$

where $\boldsymbol{u}^{(l-1)} = \sum_{i=1}^{l-1} \boldsymbol{\mathcal{C}}_{i,\boldsymbol{h}}[m_i]$ is the *cumulative vector*. It is easy to show that $s^{(V)}$ is the L2 distance of interest, i.e., $s^{(V)} = \|\boldsymbol{y} - \sum_{v=1}^{V} \boldsymbol{\mathcal{C}}_{v,\boldsymbol{h}}[m_v]\|_2^2$.

The maximum a posterior (MAP) solution can be obtained by checking all possible $\{m_1, m_2, \ldots, m_V\}$ combinations. However, this would lead to an overwhelmingly high complexity. As a low complexity alternative, we introduce the K-best decoding algorithm. In particular, for each layer, we only preserve K candidates, and prune the others. The process starts from the root of the tree with a score initialized to $s^{(0)} = 0$. In the l-th layer, the k-th surviving node in the previous layer with accumulated indices $(m_1^k, \ldots, m_{l-1}^k)$ is extended to M child nodes and the score of its m-th child, can be calculated as:

$$s^{(l)}_{m_1^k, \ldots, m_{l-1}^k, m_l} = s^{(l-1)}_{m_1^k, \ldots, m_{l-1}^k} + \|\boldsymbol{\mathcal{C}}_{l,\boldsymbol{h}}[m_l]\|_2^2$$
$$+ 2\Re(\boldsymbol{\mathcal{C}}_{l,\boldsymbol{h}}^\dagger[m_l]\boldsymbol{u}_k^{(l-1)} - \boldsymbol{\mathcal{C}}_{l,\boldsymbol{h}}^\dagger[m_l]\boldsymbol{y}), \tag{12}$$

where $\boldsymbol{u}_k^{(l-1)} = \sum_{i=1}^{l-1} \boldsymbol{\mathcal{C}}_{i,\boldsymbol{h}}[m_i^k]$. After obtaining KM metrics belonging to all the K surviving nodes in the previous layer,

we select the K smallest candidates and prune the others. By iteratively extending and pruning the tree, we can obtain K candidates at the V-th layer, where the k-th candidate can be characterized by its accumulated indices denoted by $(m_1^k, \ldots, m_V^k)$. It is also associated with its accumulated vector, $\boldsymbol{u}_k^{(V)}$, and the metric, $s_k^{(V)} \triangleq s_{m_1^k, \ldots, m_V^k}^{(V)}$.

It is worth mentioning that the decoding order of the layers makes a difference and we adopt the *per-layer* sorting in [9], where the layers with more 'reliable' candidates should be decoded earlier to prevent error propagation to the remaining layers. As a result, the true decoding order, $\mathcal{L}$, is a permutation of $[1, 2, \ldots, V]$.

We also implement 'looped K-best decoding', proposed in [9], with N_i^d extra iterations to further improve the PER performance. In particular, the looped K-best decoder takes the output of the original K-best decoding algorithm as input and outputs the updated indices of the K candidates, which can be expressed as:

$$\{(m_1^k, \ldots, m_V^k)\}_{k \in [1,K]} = \text{loopedKbest}(\\ \{(m_1^k, \ldots, m_V^k), \boldsymbol{u}_k^{(V)}, \boldsymbol{s}_k^{(V)}\}_{k \in [1,K]}, \mathcal{L}, N_i^d). \quad (13)$$

We refer the interested readers to [9] for more details of the looped K-best decoding procedure.

Finally, for the k-th candidate of the looped K-best decoder, we convert each of its V indices, $(m_1^k, \ldots, m_V^k)$ into a bit sequence, denoted by $\hat{c}_k^v, v \in [1, V]$. Then, the overall decoded bit sequence corresponding the the k-th candidate is obtained by concatenating all V bit sequences together, $\hat{c}_k = (\hat{c}_k^1, \ldots, \hat{c}_k^V)$. We apply CRC to each of the K bit sequences, $\hat{c}_k, k \in [1, K]$, in sequential order and the first bit sequence which passes the CRC will be served as the final decoded output, $\hat{c}$. If none of the K bit sequences passes the CRC, we set the error flag, T to 0, otherwise set $T = 1$. The entire CRC-aided K-best decoding algorithm is summarized in Algorithm 1. Note that we use the notation $\text{idx}(k)$ to represent the indices, $(m_1^k, \ldots, m_V^k)$ in the algorithm.

B. Iterative decoding and parameter sensing

We then illustrate the proposed iterative decoding and parameter sensing algorithm which significantly improves both the communication and sensing performance. In the standard ISAC algorithm, the BS outputs the estimated sensing parameters and the CSI *merely* using the pilot signal, and the $B \geq 1$ data packets are decoded using the estimated CSI. The main idea behind the proposed iterative algorithm is to treat the successfully decoded data packets as pilot signals, and use them to generate a more accurate channel estimation and the refined CSI will help improve the decoding performance. The overall flowchart of the proposed scheme is shown in Fig. 2 and is detailed as follows.

As shown in the left of Fig. 2, B input bit sequences, $(\boldsymbol{b}_1, \ldots, \boldsymbol{b}_B)$ are CRC encoded to produce $\boldsymbol{c}_b, b \in [1, B]$, and the transmitted symbols, $\boldsymbol{x}_b$, are generated via SPARC encoding. After passing the multi-path fading channel, the receiver has access to $\boldsymbol{y}_b, b \in [1, B]$, as well as the received pilot, $\boldsymbol{y}_p$. Since the BS has not yet decoded the data symbols, i.e., $\boldsymbol{x}_b$, it

---

Algorithm 1: CRC-aided K-best decoding algorithm with *per-layer* sorting for OFDM channel.

Input : $K, N_i^d, \boldsymbol{y}, \{\mathcal{C}_{\boldsymbol{h}}\}$
Output: $T, \hat{c}$

1 **for** $k = 1$ **to** K **do**
2    $\boldsymbol{u}(k) \leftarrow 0$ (zero accumulative vector)
3    $s(k) \leftarrow 0$ (zero score metric)
4    $\text{idx}(k) \leftarrow [\,]$ (empty candidate index)
5 $\mathcal{L} \leftarrow [\,]$ (empty decoded layer index)
6 $T \leftarrow 0$ (CRC flag)
7 %% **Original K-best decoding:**
8 **for** $j = 1$ **to** V **do**
9    $l_j \leftarrow \texttt{ChooseLayer}(\overline{\mathcal{L}})$
10    $\mathcal{L} \leftarrow [\mathcal{L}, l_j]$
11   **for** $k = 1$ **to** K **do**
12      $\boldsymbol{s}^{tmp}(k) \leftarrow s(k) - 2\Re(\boldsymbol{y}^\dagger \mathcal{C}_{l_j,\boldsymbol{h}} - \boldsymbol{u}^\dagger(k)\mathcal{C}_{l_j,\boldsymbol{h}}) + diag(\mathcal{C}_{l_j,\boldsymbol{h}}^\dagger \mathcal{C}_{l_j,\boldsymbol{h}})$
13    $[\boldsymbol{s}, \text{idx}_{new}, \text{anc}] \leftarrow \texttt{SelectNodes}(\boldsymbol{s}^{tmp}, K)$
14   **for** $k = 1$ **to** K **do**
15      $\boldsymbol{u}(k) \leftarrow \boldsymbol{u}(\text{anc}(k)) + \mathcal{C}_{l_j,\boldsymbol{h}}[\text{idx}_{new}(k)]$
16      $\text{idx}(k) \leftarrow [\text{idx}(\text{anc}(k)), \text{idx}_{new}(k)]$

17 %% **Looped K-best decoding:**
18 $\text{idx} = \texttt{LoopedKBest}(\text{idx}, \{\boldsymbol{u}_k^{(V)}, \boldsymbol{s}_k^{(V)}\}_{k \in [1,K]}, \mathcal{L}, N_i^d)$
19 $\text{outputList} \leftarrow \texttt{Reorder}(\text{idx}, \mathcal{L})$
20 %% **CRC decoding:**
21 **while** $T \neq 1$ *and* $k \leq K$ **do**
22    $\hat{c} \leftarrow \texttt{IdxToBits}(\text{outputList}(k))$
23    $T \leftarrow \texttt{CRCDecode}(\hat{c})$

---

can only produce the LMMSE estimate of the channel, denoted by $\hat{\boldsymbol{h}}^{(0)}$, using the pilot as shown in (3). Moreover, we initialize the CRC flag and the decoded bit sequences for each of the B data packets to $\{T_b = 0, \hat{c}_b = \boldsymbol{0}\}_{b \in [1,B]}$, respectively.

In the first iteration, the data symbols are decoded using $\hat{\boldsymbol{h}}^{(0)}$. The SPARC decoding process for the b-th packet can be expressed as:

$$\{T_b, \hat{c}_b\} = g(K, N_i^d, \boldsymbol{y}_b, \mathcal{C}_{\hat{\boldsymbol{h}}^{(0)}}), \quad (14)$$

where $g(\cdot)$ denotes the CRC-aided K-best decoding algorithm summarized in Algorithm 1, $T_b \in \{0, 1\}$ represents the CRC flag, and $\mathcal{C}_{\hat{\boldsymbol{h}}^{(0)}}$ is calculated as in (9). It is worth mentioning that having $T_b = 1$ does not guarantee successful decoding of the packet, i.e., $\hat{c}_b \neq \boldsymbol{c}_b$. This is because some wrongly decoded packets may also pass the CRC. We term this event as an 'outage' and the outage probability is denoted by P_o. Since P_o is typically small, it is plausible to assume that the packet with $T_b = 1$ is correctly decoded and the output bit sequence, $\hat{c}_b$, will be used to re-estimate the channel[6]. We denote the number of successfully decoded data packets in the

---

[6]It is shown in the experiment that the wrongly decoded packets that pass the CRC have little effect on the final performance.

Algorithm 2: The iterative decoding and sensing algorithm.

Input : $\boldsymbol{x}_p, \boldsymbol{y}_p, \{\boldsymbol{y}_b\}_{b\in[1,B]}, K, N_i^d, N_i, B, \mathcal{C}$
Output: $\{\hat{\boldsymbol{c}}_b\}_{b\in[1,B]}, \hat{\boldsymbol{h}}^{(N_i)}$

1   $\hat{\boldsymbol{h}}^{(0)} = \boldsymbol{R}_h(\boldsymbol{R}_h + \sigma_p^2(\boldsymbol{x}_p\boldsymbol{x}_p^\dagger)^{-1})^{-1}\boldsymbol{y}_p/\boldsymbol{x}_p$
2   $\{T_b, \hat{\boldsymbol{x}}_b\}_{b\in[1,B]} \leftarrow \boldsymbol{0}_B, \boldsymbol{0}_{B\times N}$
3   **for** $n=1$ **to** N_i **do**
4      $\mathcal{C}_{\hat{\boldsymbol{h}}^{(n-1)}} \leftarrow \text{UpdateCodebook}(\mathcal{C}, \hat{\boldsymbol{h}}^{(n-1)})$
5   ▷ Equation (9).
6   **for** $b=1$ **to** B **do**
7   **if** $T_b = 0$ **then**
8              $\{T_b, \hat{\boldsymbol{c}}_b^{(n)}\} = g(K, N_i^d, \boldsymbol{y}_b, \{\mathcal{C}_{\hat{\boldsymbol{h}}^{(n-1)}}\})$
9              $\hat{\boldsymbol{x}}_b \leftarrow \text{SPARCEncode}(\hat{\boldsymbol{c}}_b^{(n)})$
10   **else**
11   pass
12      $\boldsymbol{y}_{ext}^{(n)}, \boldsymbol{x}_{ext}^{(n)}, \boldsymbol{X}_S^{(n)} \leftarrow$
        $\text{Construct}(\boldsymbol{x}_p, \boldsymbol{y}_p, \{\boldsymbol{y}_b, \hat{\boldsymbol{x}}_b, T_b\}_{b\in[1,B]})$
13   ▷ Equation (16) and (17).
14      $\tilde{\boldsymbol{h}}^{(n)} = \boldsymbol{R}_h(\boldsymbol{R}_h + (\boldsymbol{X}_S^{(n)}\boldsymbol{X}_S^{(n)\dagger})^{-1})^{-1}\boldsymbol{y}_{ext}^{(n)}/\boldsymbol{x}_{ext}^{(n)}$
15   Estimate $(\hat{\tau}_l^{(n)}, \hat{\alpha}_l^{(n)})$ using $\tilde{\boldsymbol{h}}^{(n)}$;
16   Generate $\hat{\boldsymbol{h}}^{(n)}$ using $(\hat{\tau}_l^{(n)}, \hat{\alpha}_l^{(n)})$.

first iteration by $n_1 = \sum_{b=1}^B T_b$, with indices $\{I_1, \ldots, I_{n_1}\}$ satisfying $1 \leq I_1 < \cdots < I_{n_1} \leq B$. Each of the n_1 decoded bit sequences, $\hat{\boldsymbol{c}}_{I_i}$ are SPARC re-encoded to generate the codeword, $\hat{\boldsymbol{x}}_{I_i}$, and $\hat{\boldsymbol{x}}_{I_i} = \boldsymbol{x}_{I_i}$ holds if no outage happens. Then, the re-encoded codewords, $\hat{\boldsymbol{x}}_{I_i}$, can be treated as pilot signals known by the receiver, and the corresponding received signals, $\boldsymbol{y}_{I_b}$, are utilized to generate a refined channel estimate, which can be expressed as:

$$\tilde{\boldsymbol{h}}^{(1)} = \boldsymbol{R}_h(\boldsymbol{R}_h + (\boldsymbol{X}_S^{(1)}\boldsymbol{X}_S^{(1)\dagger})^{-1})^{-1}\boldsymbol{y}_{ext}^{(1)}/\boldsymbol{x}_{ext}^{(1)}, \quad (15)$$

where $\boldsymbol{R}_h$ is the same as in (3), $\boldsymbol{y}_{ext}^{(1)} \in \mathbb{C}^{(n_1+1)N}$ is obtained by concatenating the received pilot signal, $\boldsymbol{y}_p$, and the received data packets that pass CRC:

$$\boldsymbol{y}_{ext}^{(1)} = [\boldsymbol{y}_p^\top, \boldsymbol{y}_{I_1}^\top, \ldots, \boldsymbol{y}_{I_{n_1}}^\top]^\top, \quad (16)$$

and $\boldsymbol{x}_{ext}^{(1)}$ is obtained in the same way. The matrix, $\boldsymbol{X}_S^{(1)}$ is defined as:

$$\boldsymbol{X}_S^{(1)} = [\boldsymbol{x}_p/\sigma_p, \hat{\boldsymbol{x}}_{I_1}/\sigma, \ldots, \hat{\boldsymbol{x}}_{I_{n_1}}/\sigma], \quad (17)$$

where σ denotes the noise power for the data packets.

After obtaining $\tilde{\boldsymbol{h}}^{(1)}$ from the LMMSE channel estimator, we update the sensing parameters, $(\hat{\tau}_l^{(n)}, \hat{\alpha}_l^{(n)})$ as in Section II-B. The frequency response, $\hat{\boldsymbol{h}}^{(1)}$ corresponding to the updated sensing parameters, will be used in the second iteration.

It is worth mentioning that, for the second iteration, we only need to decode the remaining $(B-n_1)$ data packets using $\hat{\boldsymbol{h}}^{(1)}$, while the n_1 successfully decoded packets, $(\hat{\boldsymbol{c}}_{I_1}, \ldots, \hat{\boldsymbol{c}}_{I_{n_1}})$ remain the same. The iterative decoding and sensing process

terminates if the number of iterations reaches N_i, or all the B data packets pass CRC.

We evaluate the performance of the proposed iterative algorithm by calculating the PER and the MSE defined in (4) and (7), respectively. We summarize the entire iterative decoding and sensing procedure in Algorithm 2.

IV. NUMERICAL EXPERIMENTS

A. Parameter Settings

Unless otherwise specified, we consider short packet transmission where each data packet is comprised of 13 information bits with an 11-bit CRC whose generator polynomial is $x^{11}+x^{10}+x^9+x^5+1$. The parameters of the SPARC are set to $V=3, M=256, N=32$. The number of OFDM subcarriers is $N=32$ and $L=3$ paths are considered. Without loss of generalizability, we assume $\alpha_l \in \mathcal{CN}(0, \frac{1}{L}), l \in [1, L]$ and $n_l = l$, i.e., the delay occupies the first L taps. Finally, for the SPARC decoding, we set the number of surviving candidates, $K = 16$ at each layer and set the number of extra iterations, $N_i^d = 3$.

B. Performance Evaluation

1) Performance improvement w.r.t. N_i: We first illustrate the improvement brought by the number of iterations. In this simulation, different pilot SNR values, $\text{SNR}_p \in \{-3, 1, 5, 9\}$ dB are considered and the number of pilot frames and data packets are set to 1 and $B = 6$, respectively. The SNR of the data packets is fixed at 9 dB. The PER and MSE performances are evaluated after collecting enough number of packet errors. It can be seen from Fig. 3 (a) and (b) that both the PER and the MSE improve significantly w.r.t N_i. In particular, Fig. 3 (a) shows for all SNR_p values, the PER performance converges with merely 3 iterations. We can also observe that the PER performance of the SPARC with $\text{SNR}_p = 9$ dB and $N_i = 4$ nearly approaches the PER performance of the SPARC with perfect pilot.

We also provide the PER performance of the Polar baseline to outline the effectiveness of the proposed SPARC. The Polar baseline utilizes the same 11-bit CRC and adopts successive cancellation list decoding algorithm. In particular, the 13 information bits are first CRC encoded and the Polar encoder encodes the length-24 input bit sequence into a bit sequence with 64 bits which is modulated to generate 32 QPSK symbols for transmission. The decoded bit sequence is obtained after the MMSE equalization and Polar decoding. As can be seen in Fig. 3 (a), the proposed SPARC outperforms the Polar baseline in terms of PER.

Fig. 3 (b) manifests the MSE of the parameters, (α_l, τ_l), w.r.t. N_i. The MSE is large when $N_i = 0$ which is due to the fact that we only use one $\boldsymbol{x}_p$ frame to estimate the parameters. When N_i grows, a larger number of data packets are successfully decoded and the LMMSE channel estimator in (15) produces more accurate channel estimates leading to improved MSE performance.
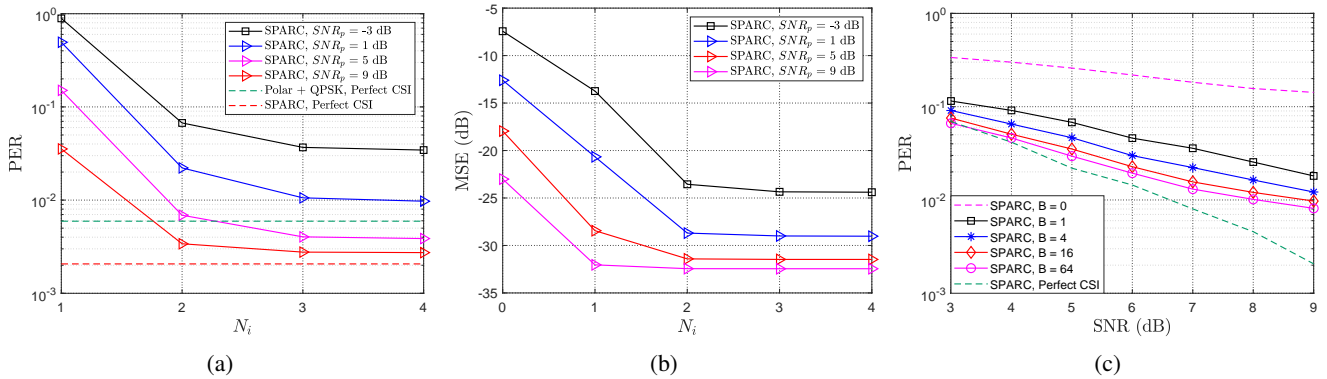
Fig. 3: Performance evaluation of the proposed coded ISAC system: (a) & (b) the PER and MSE performances versus the number of iterations, N_i, with different pilot SNR values and $B = 6$; (c) the PER performance with different numbers of blocks, B, where $\text{SNR}_p = 1$ dB and $N_i = 4$.
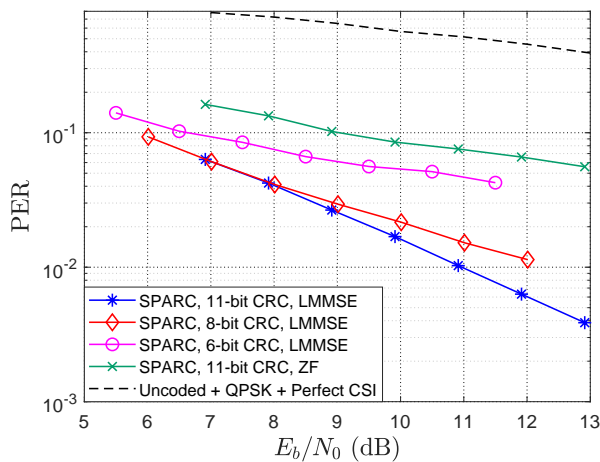

Fig. 4: The PER performance of the SPARC with different numbers of CRC bits and different channel estimation methods are evaluated. We also provide an uncoded benchmark to outline the effectiveness of the channel codes. It is worth emphasizing that we adopt E_b/N_0 as the x-axis for a fair comparison of the schemes with different spectrum efficiencies.

2) The effects of different number of data packets: we investigate the effect of different number of data packets, B, on the system performance. In this simulation, the pilot SNR is fixed at $\text{SNR}_p = 1$ dB, while B is selected from $B \in \{1, 4, 16, 64\}$. Intuitively, increasing B enhances the probability of correctly decoding a larger number of data packets, which can then serve as additional pilot symbols, thereby improving the accuracy of channel estimation. However, a larger B also introduces higher latency, as the latency scales proportionally with B. Depending on the specific application, it is important to determine an optimal B that balances the trade-off between decoding latency and PER performance.

As can be seen in Fig. 3 (c), the PER performance improves rapidly from $B = 0$ to $B = 4$ yet it nearly ceases to improve when $B \geq 16$. It is also shown in the figure that there is a gap between $B = 64$ and the SPARC with perfect CSI which is due

TABLE I: The outage probabilities, P_o, for three CRC settings with different SNR values.

SNR (dB)	3	6	9
P_o w/ 6-bit CRC	0.102	0.058	0.040
P_o w/ 8-bit CRC	0.028	0.015	0.009
P_o w/ 11-bit CRC	2.2×10^{-3}	1.7×10^{-3}	1.2×10^{-3}

to the CRC outage: the wrong SPARC re-encoded codewords would degrade the channel estimate which hinders the final PER performance. This will be verified in the subsequent simulations concerning the outage probability, P_o.

3) Ablation studies: Finally, we provide ablation studies for a comprehensive understanding of the proposed iterative decoding and sensing system. In particular, we fix the SPARC parameters, i.e., $(V = 3, M = 256, N = 32)$ and change different CRC settings as well as the channel estimation methods. In particular, we consider 6-bit and 8-bit CRC with generator polynomials, $x^6 + x^5 + 1$ and $x^8 + x^2 + x + 1$, respectively. The PER performance of the zero-forcing (ZF) channel estimation method with 11-bit CRC is evaluated as well as the PER performance of the uncoded QPSK symbols with perfect CSI. For all the schemes, we set the number of blocks, B, to 6 and the pilot SNR, $\text{SNR}_p = 5$ dB. It is worth mentioning that, to provide a fair comparison for the schemes with different CRC lengths (leading to different spectrum efficiencies), we use E_b/N_0 instead of SNR as the x-axis.

As shown in Fig. 4, without the aid of channel codes, the PER of the uncoded QPSK symbols is much higher than that using channel codes. Moreover, a significant gain is observed by comparing the PER performance between the LMMSE channel estimator with the ZF counterpart. It is also shown that having a shorter CRC would harm the system performance, this is due to the fact that the outage probabilities, P_o, for both the 6-bit and 8-bit CRC settings are relatively high as shown in Table I. This would lead to wrong SPARC re-encoded symbols, $\hat{x}_b$, and harms the subsequent channel estimation performance. The 11-bit CRC has a much smaller P_o, thus, it has the best PER performance. It is also shown in Table

I that P_o is decreasing w.r.t. SNR as the proposed SPARC decoding algorithm produces more reliable bit sequences with higher SNR.

V. Conclusion

In this paper, a novel integrated passive sensing and communication system is proposed for OFDM system where the BS performs parameter sensing and channel decoding simultaneously. CRC-aided SPARC code is adopted to protect the information bits from channel distortion. The BS adopts a novel iterative decoding and sensing algorithm where the correctly decoded data packets will be used to improve the sensing performance, then, the improved parameter estimates will in turn help to decode more data packets. Extensive simulations are carried out to verify the gain achieved by the iterative decoding and sensing algorithm. We also provide an ablation study concerning different channel estimation methods and different numbers of CRC bits for a comprehensive understanding of the proposed scheme.

References

[1] F. Liu, C. Masouros, A. P. Petropulu, H. Griffiths, and L. Hanzo, "Joint radar and communication design: Applications, state-of-the-art, and the road ahead," *IEEE Transactions on Communications*, vol. 68, no. 6, pp. 3834–3862, 2020.

[2] F. Liu, Y. Cui, C. Masouros, J. Xu, T. X. Han, Y. C. Eldar, and S. Buzzi, "Integrated sensing and communications: Toward dual-functional wireless networks for 6G and beyond," *IEEE Journal on Selected Areas in Communications*, vol. 40, no. 6, pp. 1728–1767, 2022.

[3] K. Meng, C. Masouros, A. P. Petropulu, and L. Hanzo, "Cooperative ISAC networks: Opportunities and challenges," *IEEE Wireless Communications*, pp. 1–8, 2024.

[4] W. Jiang, D. Ma, Z. Wei, Z. Feng, P. Zhang, and J. Peng, "ISAC-NET: Model-driven deep learning for integrated passive sensing and communication," *IEEE Transactions on Communications*, pp. 1–1, 2024.

[5] J. Hu, I. Valiulahi, and C. Masouros, "ISAC receiver design: A learning-based two-stage joint data-and-target parameter estimation," *IEEE Wireless Communications Letters*, pp. 1–1, 2024.

[6] S. Aditya, O. Dizdar, B. Clerckx, and X. Li, "Sensing using coded communications signals," *IEEE Open Journal of the Communications Society*, vol. 4, pp. 134–152, 2023.

[7] R. Zhang, B. Shim, W. Yuan, M. D. Renzo, X. Dang, and W. Wu, "Integrated sensing and communication waveform design with sparse vector coding: Low sidelobes and ultra reliability," *IEEE Transactions on Vehicular Technology*, vol. 71, no. 4, pp. 4489–4494, 2022.

[8] A. Joseph and A. R. Barron, "Fast Sparse Superposition Codes Have Near Exponential Error Probability for $R < \mathcal{C}$," vol. 60, no. 2, pp. 919–942, 2014.

[9] C. Bian, C.-W. Hsu, C. Lee, and H.-S. Kim, "Learning-based near-orthogonal superposition code for MIMO short message transmission," *IEEE Transactions on Communications*, vol. 71, no. 9, pp. 5108–5123, 2023.

[10] H. Kim, "HDM: Hyper-Dimensional Modulation for Robust Low-Power Communications," in *2018 IEEE International Conference on Communications (ICC)*, May 2018, pp. 1–6.

[11] C. Bian, M. Yang, C.-W. Hsu, and H.-S. Kim, "Deep learning based near-orthogonal superposition code for short message transmission," in *ICC 2022 - IEEE International Conference on Communications*, 2022, pp. 3892–3897.